F47 — Cyclotron frequency in a Penning trap

"Stored and Cooled Ions" Division
at the Max-Planck Institute for Nuclear Physics
led by Klaus Blaum

November 3, 2026

1 Introduction

The mass m is closely related to the energy E via the famous relationship

$$E = mc^2 \quad .$$

This relationship can be used to convert mass measurements to energy measurements. For example, the mass difference between the mother nucleus and daughter nucleus in a radioactive decay is equivalent to the decay energy. The measurement of such energies is important in many areas of physics:

Astrophysics: One of the "11 Science Questions for the New Century" that were formulated by the NRC in 2002 was: "How were the elements from iron to uranium made?" Mass spectrometry provides key parameters (e.g. neutron separation energies) for building models that explain how nuclei are formed in supernovas and stars.

Nuclear physics: The measurement of nuclear masses helps to improve mass models. The masses of radioactive nuclei are of particular interest. One goal is to find the "island of stability", which is predicted by many different models of nuclear masses.

Tests of QED: Measuring the binding energy of the $1s$-electron in hydrogen-like uranium (U^{91+} allows to test QED in strong fields[1]. The ionization energy of U^{91+} from the ground state is approximately 200 keV and far out of the reach of laser spectroscopy. High precision mass measurements allow to measure this energy.

Neutrino physics: The determination of the neutrino mass is an active research field in particle physics and astrophysics. A precise measurement would yield an important parameter in theories beyond the Standard Model of physics. The neutrino mass is also needed for estimating the energy that is required for neutrino production during the big bang. Penning traps can help to measure this value by determining β-decay energies. The difference between the total energy of a β-decay and the maximum energy that the β-electrons can have (provided by a separate measurement) is equal to the mass energy of the $\bar{\nu}_e$- neutrino.

Penning traps are useful tools in mass spectrometry, but they can also be used to measure other properties of charged particles, such as magnetic moments or electric dipole moments.

Table 1.1: Applications of mass spectrometry and relative mass uncertainty that is needed [Blaum, 2006].

Field	Rel. mass uncert.
Chemistry: identification of molecules	$10^{-5} - 10^{-6}$
Nuclear physics: shells, sub-shells, pairing	10^{-6}
Nuclear fine structure: deformation, halos	$10^{-7} - 10^{-8}$
Astrophysics: r-process, rp-process, waiting points	10^{-7}
Nuclear mass models and formulas: IMME	$10^{-7} - 10^{-8}$
Weak Interaction studies: CVC hypothesis, CKM unitarity	10^{-8}
Atomic physics: binding energies, QED	$10^{-9} - 10^{-11}$
Metrology: fundamental constants, CPT	$< 10^{-10}$

[1] The electric field near the uranium nucleus is one of the strongest available electrostatic fields (cf. Schwinger limit).

2 Theory[1]

2.1 Cyclotron motion

When a particle with mass m and charge q moves through a magnetic field $\vec{B}$, it experiences the Lorentzian force

$$\vec{F}_\mathrm{L} = q\,\vec{v} \times \vec{B} \quad .$$

In the special case $\vec{v} \perp \vec{B}$, the particle's trajectory will be a circle (Fig. 2.1, left). In the more general case, $\vec{v}$ has a component parallel to the magnetic field, and the trajectory is a spiral. By setting $\vec{F}_\mathrm{L}$ equal to the centripetal force, you can quickly show that the frequency of the circular motion is independent of the velocity:

$$\omega_\mathrm{c} = \frac{q}{m} B \quad . \tag{2.1}$$

This frequency is called the **free cyclotron frequency**. The basis of Penning trap mass spectrometry is to determine the cyclotron frequencies of two different particles in the same magnetic field $\vec{B}$. When the ratio of these frequencies is calculated, the magnetic field cancels out and the charge ratio reduces to an integer fraction. The frequency measurement can therefore be used to calculate a mass ratio:

$$\frac{\omega_{\mathrm{c}_1}}{\omega_{\mathrm{c}_2}} = \frac{q_1}{q_2}\frac{m_2}{m_1} \quad . \tag{2.2}$$

By using a reference ion with precisely known mass, the mass of the other particle can be determined. Charged $^{12}\mathrm{C}^{n+}$ ions are particularly well suited as reference ions because the mass of the neutral $^{12}\mathrm{C}$ atom defines the unified atomic mass unit u exactly. The mass of the ion can then be calculated from the mass of the neutral atom by subtracting the masses of the removed electrons and adding the corresponding ionization energies divided by c^2. Both the electron mass and the relevant ionization energies are known with sufficient precision that the resulting mass of the carbon ion can be used as a highly accurate reference.

State-of-the-art superconducting magnets can be carefully tuned to have a magnetic field that changes only 1 part in 10^8 over a $1\,\mathrm{cm}^3$ region in the center. When a charged particle is inserted into such a field, it orbits around the field lines (in other words, it is trapped radially), but it is free to drift axially, along the field lines, out of the homogeneous part of the magnetic field. This considerably reduces the useful time in which the particle can be studied or in which its cyclotron frequency can be determined.
The idea of a Penning trap is to have a weak, electric field that axially pushes the particles towards a defined point. But before describing this field, let us consider the motion of particles in strong $\vec{B}$-fields with simultaneous, weak $\vec{E}$-fields.

2.2 Guiding center motion

If in addition to the magnetic field $\vec{B}$ there is a weak[2] electric field $\vec{E}$, the trajectory of charged particles can be separated into a fast cyclotron motion, caused by $\vec{B}$, and a slow

[1] Parts of this chapter are based on the doctoral thesis by Martin Höcker.
[2] Weak meaning that the electric forces are much smaller than the magnetic forces.

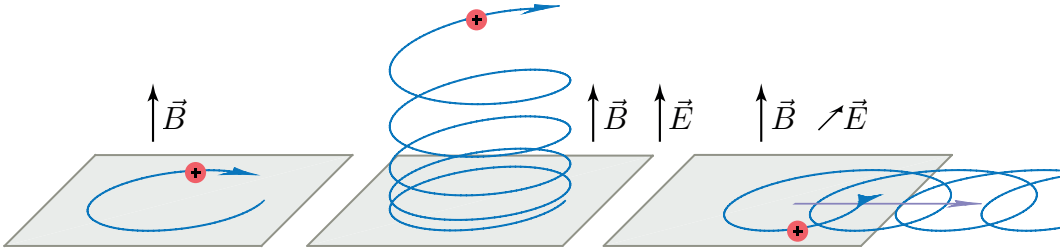


Figure 2.1: Motion of a charged particle in a magnetic field (left), in magnetic field parallel to an electric field (center), and a magnetic field orthogonal to an electric field (right).

drift of the center of the cyclotron motion, caused by $\vec{E}$. The center of the cyclotron motion is also called the guiding center.
For example: If $\vec{E} \parallel \vec{B}$, the radial motion is undisturbed, and the particle is accelerated axially, along the field lines. The trajectory is a spiral that has more and more space between its loops (Fig. 2.1, center).
When $\vec{E} \perp \vec{B}$, the particle accelerates and decelerates as it moves on its cyclotron orbit. The radius of the orbit grows as the particle moves in the direction of $\vec{E}$ and shrinks again during the other half of the orbit. This causes the center of the cyclotron motion to drift sideways, orthogonal to both the electric and the magnetic field (Fig. 2.1, right). This drift is called the E-cross-B drift.
The general case can be described by a superposition of $\vec{E}_{\parallel}$ and $\vec{E}_{\perp}$.
We now have the tools to describe the motion of charged particles in a Penning trap.

2.3 Penning trap motion

This section gives a qualitative description of the motion. For a more rigorous quantitative treatment, see Sec. 2.5. By convention, the magnetic field points towards the z-direction, so that $\vec{B} = B\vec{e}_z$. The electric field that leads to something called Penning trap can then be written as

$$\vec{E} = c \begin{pmatrix} x/2 \\ y/2 \\ -z \end{pmatrix} \quad , \tag{2.3}$$

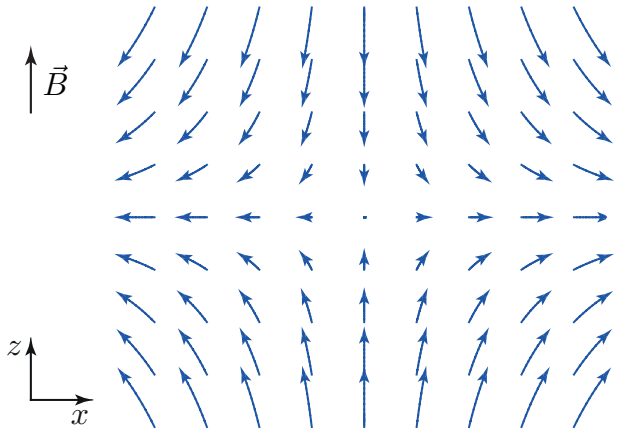


Figure 2.2: Cut-view of the electric field inside a Penning trap.

with some arbitrary constant c (Fig. 2.2). The important part is happening in the E_z-component: Assuming the signs of c and charge q are the same, the electric field pushes the particles towards $z = 0$. Since this force is proportional to the z-displacement, like in a spring, the z-motion is a harmonic oscillation (Fig. 2.3) with the **axial frequency** ω_z.
The field in the xy-plane (the "radial" plane) is a necessary trade-off, as dictated by Gauss's law: The field lines that are coming in towards the trap center in the z-direction, need to come out somehow. In an ideal Penning trap, the radial components of the $\vec{E}$-field point evenly away from the trap center.
The radial components of $\vec{E}$ pull the particles away from the trap center. As they accelerate outwards, their cyclotron orbit increases. When the cyclotron motion takes the particles back towards the trap center, their cyclotron orbit decreases. In total, the center of the cyclotron motion (the guiding center) performs a slow E-cross-B-drift around the center of the trap (Fig. 2.3). In Penning trap terms, this slow drift is called the magnetron motion and behaves like a harmonic oscillator with the so-called **magnetron frequency** ω_-.
The drift of the guiding center slightly reduces the frequency of the fast cyclotron motion, see Sec. 2.5. This other motion in the radial plane moves with a frequency ω_+, called the **modified cyclotron frequency**. It is important to point out that the magnetron motion is unstable[3]! The particles sit on a potential hill in the radial plane. If there are any damping processes, such as collisions with background gas, the particles roll down the potential hill and are lost. In cryogenic traps that are cooled to 4 K, particles can easily be stored for years and longer [Blaum et al., 2009], but in the room-temperature Penning trap of this experiment, the storage times are on the order of 100 ms.

2.4 Penning trap electrodes

The electric field $\vec{E}$ of a perfect Penning trap corresponds to the potential

$$\Phi = \frac{c}{2}\left(\frac{-\rho^2}{2} + z^2\right) \quad , \tag{2.4}$$

[3]It can be argued that the term Penning "trap" is a misnomer, but "Penning arbitrarily long storage device" does not have the same ring to it.

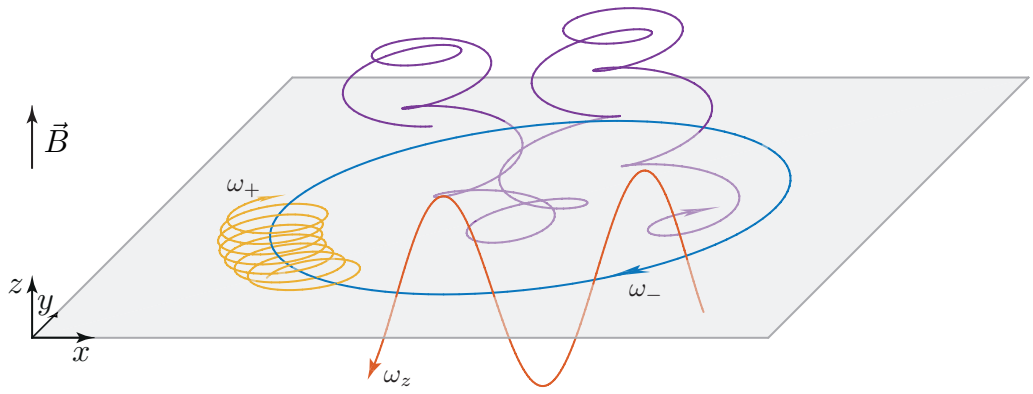


Figure 2.3: Motion of a positively charged particle in a Penning trap. The motion consists of the slow magnetron drift around the trap center ω_- (blue), the axial motion ω_z (red), and the modified cyclotron motion ω_+ (yellow). The superposition of all three motions is shown in purple.

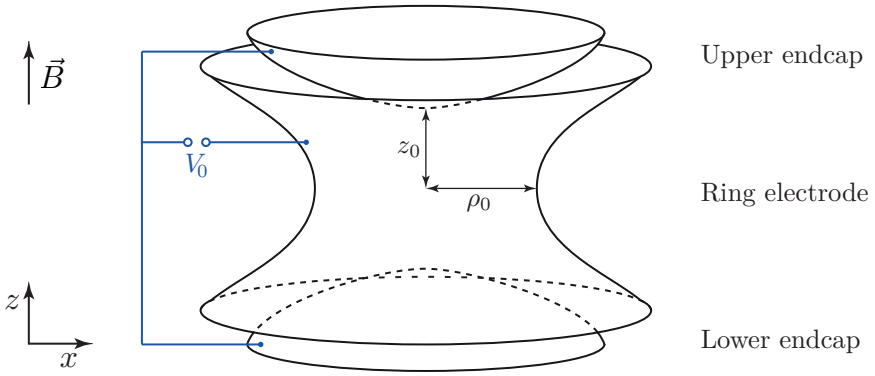


Figure 2.4: Hyperbolic Penning trap electrodes.

where $\rho^2 = x^2 + y^2$. To create this potential inside the Penning trap, there are three cylindrically symmetric electrodes that follow the equipotential lines of Φ: Two electrodes follow the contours

$$z(\rho) = \pm\sqrt{z_0^2 + \frac{\rho^2}{2}} \quad , \tag{2.5}$$

with z_0 as the closest point to the trap center.
These electrodes are called the endcaps (Fig. 2.4). Both endcaps are held at the same potential. The third electrode, called the ring electrode, follows the contour:

$$\rho(z) = \pm\sqrt{\rho_0^2 + 2z^2} \quad , \tag{2.6}$$

with ρ_0 being the distance between trap center and ring electrode. Let V_0 be the voltage between the ring electrode and the endcaps. Then the potential in the trap can be written as:

$$\Phi(\rho, z) = \frac{V_0}{z_0^2 + \frac{1}{2}\rho_0^2}\left(z^2 - \frac{1}{2}\rho^2\right) \overset{\text{this trap}}{=} \frac{V_0}{2z_0^2}\left(z^2 - \frac{1}{2}\rho^2\right) \tag{2.7}$$

2.5 Penning trap frequencies

To quantify our qualitative understanding of the Penning trap trajectories, we have to solve the equations of motion

$$\ddot{\vec{r}} = \frac{q}{m}\left(\dot{\vec{r}} \times \vec{B} + \vec{E}\right) \quad . \tag{2.8}$$

With $\vec{B} = B\vec{e}_z$ and Equation 2.7 for the potential $\Phi(\rho, z)$ that defines the electric field $\vec{E} = -\vec{\nabla}\Phi$, we can rewrite this as

$$\begin{pmatrix} \ddot{x} \\ \ddot{y} \\ \ddot{z} \end{pmatrix} = \frac{q}{m}B\begin{pmatrix} \dot{y} \\ -\dot{x} \\ 0 \end{pmatrix} + \frac{qV_0}{2mz_0^2}\begin{pmatrix} x \\ y \\ -2z \end{pmatrix} \quad . \tag{2.9}$$

The z-component of this differential equation is independent of the radial components, and it has the same structure as the equation of an undamped, harmonic oscillator. It is solved by

$$z(t) = \hat{z}_0 e^{i\omega_z t} \quad \text{with} \quad \boxed{\omega_z = \sqrt{\frac{qV_0}{mz_0^2}}} \quad . \tag{2.10}$$

The frequency ω_z is called the **axial frequency**. Using the above definition for ω_z and Equation 2.1 for ω_c, the radial equations of motion can be written as

$$\begin{pmatrix} \ddot{x} \\ \ddot{y} \end{pmatrix} = \omega_c \begin{pmatrix} \dot{y} \\ -\dot{x} \end{pmatrix} + \frac{1}{2}\omega_z^2 \begin{pmatrix} x \\ y \end{pmatrix} \quad . \tag{2.11}$$

These equations can be solved by introducing the function $u(t) = x(t) + iy(t)$. With the help of this function, the radial equations of motion can be reformulated as

$$\ddot{u} = -i\omega_c \dot{u} + \frac{1}{2}\omega_z^2 u \quad . \tag{2.12}$$

Guessing a solution of the form $u(t) = u_0 e^{-i\omega t}$ leads to two independent solutions with the frequencies

$$\boxed{\omega_\pm = \frac{1}{2}\left(\omega_c \pm \sqrt{\omega_c^2 - 2\omega_z^2}\right)} \quad . \tag{2.13}$$

The frequency ω_+ is the faster frequency. This frequency is often called the **modified cyclotron frequency**, because for typical trap parameters, it is only slightly smaller than the free space cyclotron frequency ω_c. The other frequency, ω_-, is called the **magnetron frequency**. In order for the trajectory to be stable, the frequencies must be real-valued. This is only the case if $\omega_c^2 > 2\omega_z^2$. This requirement is equivalent to

$$B > \sqrt{2\frac{m}{q}\frac{V_0}{z_0^2}} \quad . \tag{2.14}$$

In other words, if the voltage between the trap electrodes is too big, then the electric forces become too large and the ions are no longer contained radially by the magnetic field. This is called the stability limit. In typical Penning traps, $\omega_- \ll \omega_z \ll \omega_+ < \omega_c$ [Blaum, 2006]. The magnetron frequency ω_- may become larger than ω_z, but this is only true if the trap is operated dangerously close to the stability limit. The fact that the motion of particles in a Penning trap can be broken down into three independent, harmonic modes is very important from a practical standpoint: It ensures that the frequencies can be measured separately and that the measurements do not depend on difficult-to-control initial conditions. The free space cyclotron frequency ω_c can easily be calculated from the trap eigenfrequencies ω_+, ω_-, and ω_z. There are two ways to do it: Either by using the sideband relation

$$\boxed{\omega_c = \omega_+ + \omega_-} \quad , \tag{2.15}$$

or by using the invariance-relation [Brown and Gabrielse, 1982], which is independent against trap imperfections

$$\boxed{\omega_c^2 = \omega_+^2 + \omega_-^2 + \omega_z^2}. \tag{2.16}$$

These relationships can easily be verified using the results of Equation 2.13 and Equation 2.10. In ideal Penning traps, they give identical results. One further relationship is quite useful when calculating one frequency from two measured frequencies:

$$\omega_+\omega_- = \frac{1}{2}\omega_z^2 \quad . \tag{2.17}$$

This follows directly from Equation 2.13.

2.6 Real Penning traps

In a real Penning trap, the convenient separation of the particle motion into three independent, harmonic modes is not strictly true. Imperfections lead to frequency offsets, to energy dependent frequency shifts (each frequency depends on the energies of all modes) and to coupling (energy exchange) between the modes. Relevant imperfections are:

- Particle interactions. If there is more than one charged particle in the Penning trap, particle interactions lead to chaotic frequency shifts and couplings. High precision Penning traps are designed to work with single ions, or with at most two ions in the trap. The interactions in the electron cloud of the FP-experiment are the biggest limitation of this device.
- Misalignment between $\vec{B}$ and $\vec{E}$. This can happen when the trap electrodes are tilted with respect to the magnet. In Penning traps used for mass spectrometry, typical frequency shifts are on a 10^{-7}-level, but it can be shown that this shift cancels out when using Equation 2.16 to calculate ω_c.
- Ellipticity of the $\vec{E}$ field, where the radial components of $\vec{E}$ are stronger in one direction than the other. This affects measurements on a 10^{-10}-level.
- Cylindrically symmetric $\vec{E}$-field imperfections. When, for example, E_z is not perfectly proportional to z but additionally also depends on z^3, then the trapped particles' z-oscillation has the characteristics of a "stiffening" (or "weakening", depending on the sign) spring, and the axial frequency changes as a function of amplitude. Relevant on a 10^{-8}-level
- Cylindrically symmetric $\vec{B}$-field imperfections. They lead to similar effects as the $\vec{E}$-field imperfections, but are typically relevant on a 10^{-10}-level.
- Relativistic shifts. These are especially important for light particles. For light ions, the reduced cyclotron frequencies are typically shifted on a 10^{-10}-level
- Image charges in the trap electrodes. Image charges always pull the charged particles to the closest electrode, away from the trap center. This modifies the equations of motions and is relevant on a 10^{-10}-level.

Most of these frequency shifts are energy dependent. Current research in Penning trap mass spectrometry pushes for lower motional amplitudes (lower ion energy), smaller trap imperfections, and better characterization of the remaining shifts. The Penning trap used in this experiment consists of a stack of five cylindrical electrodes, which reproduces a symmetric and nearly perfect quadrupole-like potential [Gabrielse et al., 1989] which can be expanded as

$$\Phi(z,\rho) = V_R \sum_{n=0}^{\infty} C_n \left(\frac{r}{d}\right)^n P_n(z/r) \overset{\text{this trap}}{\simeq} V_R C_2 \left(z^2 - \frac{1}{2}\rho^2\right) \quad . \tag{2.18}$$

Where V_R is the voltage applied to the trap electrodes, $r = \sqrt{\rho^2 + z^2}$, P_n are the Legendre Polynomials, d is the characteristic trap dimension $d^2 = 1/2\left(z_0^2 + 0.5\rho_0^2\right)$ By tuning the correction electrodes with respect to the ring electrode (see Fig. 2.5), the higher order corrections C_4 and C_6 can be set to zero. Questions:

- What is a Penning trap, what does it look like? What fields are present?
- What is the free cyclotron frequency and how is it derived (formulae)?
- What are the eigenmotions of a trapped particle in a Penning trap (names, type of movement, not exact formulae) and what important parameters do they depend on?

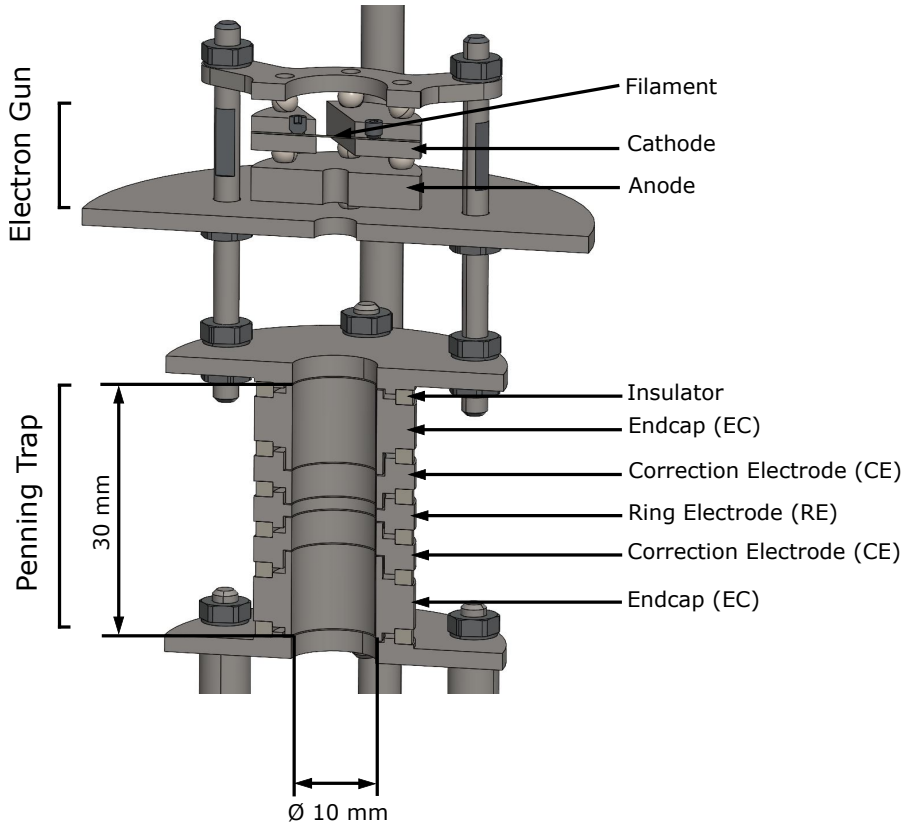


Figure 2.5: Cylindrical Penning trap electrodes, CAD model.

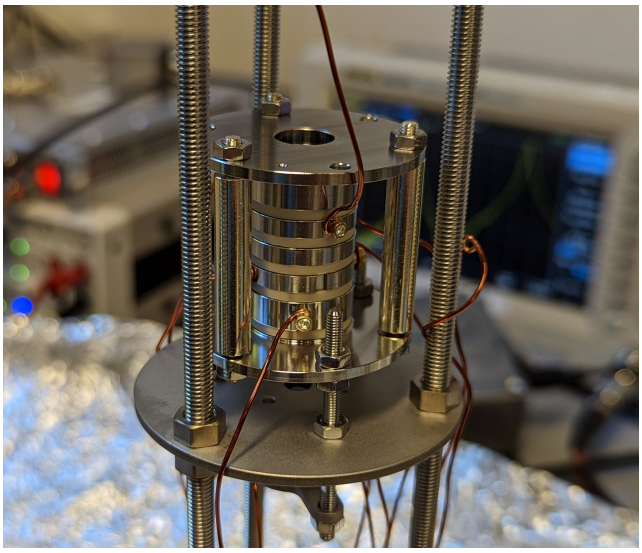


Figure 2.6: Cylindrical Penning trap electrodes, real setup.

3 Detection and Manipulation

3.1 Detecting electrons

When an electron sits motionless inside the trap, electrostatic induction causes *image charges* to form on the trap electrodes. When the electron moves, the image charges move as well. This change in charge is per definition a current $I = dQ/dt$ and is referred to as *image current*. The oscillating movement of the electrons in the trap therefore cause an AC-signal. The radial motion of trapped electrons leads to an image current that mostly flows in the ring electrode. Since the ring electrode is rotationally symmetric, this current can flow freely and does not lead to a measurable voltage drop across the ring electrode. On the other hand, the image current of the axial motion mostly flows between the endcaps, and depending on the connection (impedance) between the endcaps, causes a voltage that can be measured. The image current is low ($I \sim 10^{-12}A$), and according to Ohm's law,

$$V = ZI \quad , \tag{3.1}$$

we need a high impedance ($|Z| \sim 10^6\Omega$) for a measurable voltage drop ($V \sim 10^{-6}V$). To achieve this we could connect a 1 MΩ resistor between the endcaps and then measure the voltage drop across the resistor. However, the traps have a self-capacitance C_{eff} of several pF, which is electrically parallel to the resistor we would connect. Therefore connecting a resistor would actually decrease Z, since it will be connected in parallel. At (for electrons) typical axial frequencies of a few tens of MHz, the overall impedance is dominated by C_{eff}, and is only a few kΩ. We can solve the problem by connecting an inductor L_{res} across the endcaps

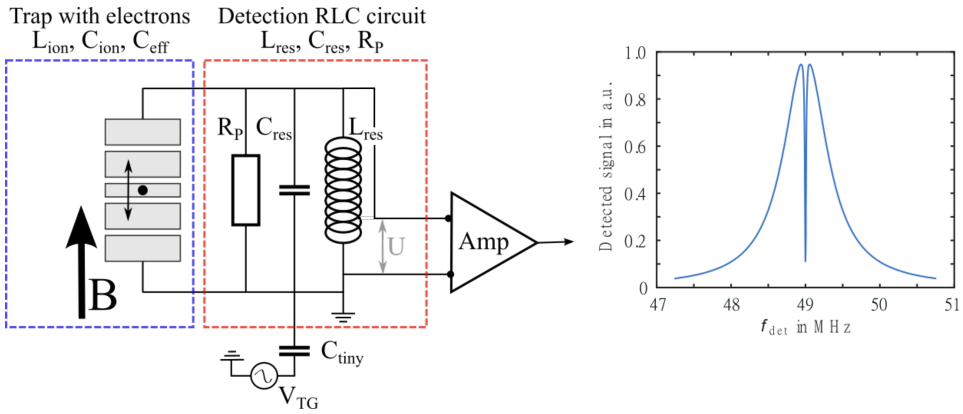


Figure 3.1: (Left) The axial ion movement induces image currents which are picked up by a RLC-circuit. The ion can be modelled as inductance and capacitance in parallel to the RLC-circuit. (Right) On resonance, the ion is detected on the resonator as dip signal. The coil is excited through a small capacitance C_{tiny}. When the ring voltage is carefully adjusted so that $\omega_z = \omega_{RLC}$, then the electrons short out the excitation signal [Ulmer et al., 2016].

(Fig. 3.1). The self-capacitance of the trap C_{eff}, the inductor L_{res}, and the resistive losses R_P of the inductor form an RLC-circuit. You can show that the impedance is maximal, and real, at a frequency of $\omega_{RLC} \approx \frac{1}{\sqrt{L_{\text{res}} C_{\text{eff}}}}$ (Fig. 3.2). The z-oscillation of the trapped particles

acts as a current source parallel to the trap capacitance C_{eff}. If the particles oscillate with ω_z near ω_{RLC}, their image current causes a measurable voltage drop across the coil. As a side effect, the voltage drop also back-acts on the moving charges and damps their motion, until they are in thermal equilibrium with the RLC-circuit. When new electrons are loaded into the experiment, they start out hot and therefore appear as a peak on top of the frequency spectrum of the detection circuit. However, they quickly cool down and the peak disappears. Therefore, we use a different method in order to detect them (see Fig. 3.1). We use a device that sends sinusoidal signals of different frequencies through the circuit and measures the amplitudes of the returned waves after they went around in the circuit (called network analyzer). Just like how the motion of the trapped electrons create an induced current at the circuit, current running through the circuit applies forces on the trapped electrons. We set the electron's axial oscillation frequency ω_z to be the same as the resonance frequency of the circuit ω_{RLC} (try to think how we can do that). We then send signals of different frequencies through the circuit. Most of these signals will apply forces which are non-resonant with the electron's axial motion. Therefore they will not excite the electrons much. (Also, these signals will mostly decay in the circuit anyhow except if they are resonant with the detection circuit). However, if we send a signal with the same frequency as the other two (so that

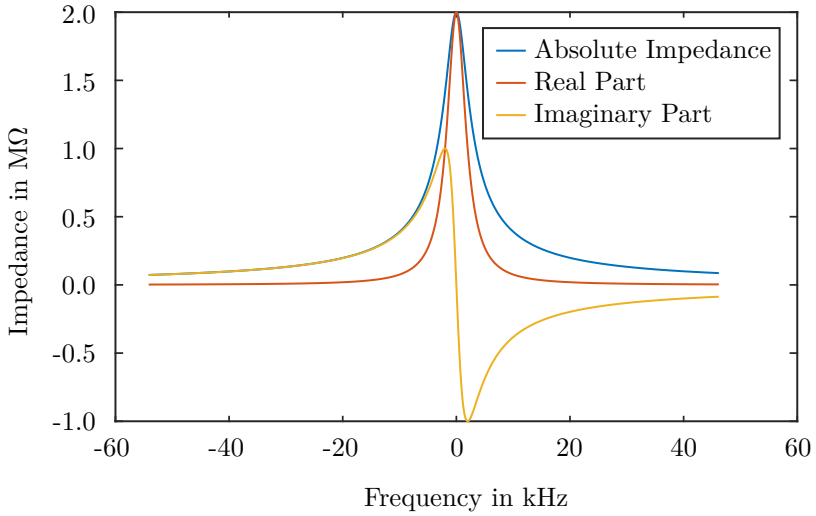


Figure 3.2: The impedance of a parallel RLC circuit for R=200kohm, L=79uH and C=22pF as a function of the angular frequency.

$\omega_{\text{signal}} = \omega_z = \omega_{RLC}$), much of its amplitude will be spent on exciting the motion of the electrons, and the returned signal will be low in amplitude. We will then see a dip in the spectrum for this frequency. This is how we can see that we have electrons in the trap - By measuring a dip in the spectrum. By the way, if the axial frequency is not close enough to the circuit's resonance frequency, the impedance will have a non-negligible imaginary component and as a result instead of a dip we will get a peak and then a dip (a dispersion curve, see Fig. 3.2)

An alternative explanation:
When the resonance frequency of the electrons, the resonance frequency of the circuit, and the frequency of the signal we send through the circuit are all identical, a significant image current flows through the electrons across the endcaps. This image current provides an additional path for the signal to flow, and it typically has a much lower impedance than the RLC circuit. The electron cloud then acts as a short and the voltage drop on the RLC circuit is reduced, producing a dip.
Note that the device sending the signals throughout the circuit is not connected directly,

rather it is connected to the circuit through a capacitor with very small capacitance (1 pF). The capacitor is there to allow a voltage difference between the signal generating device and the circuit, otherwise the signal generating device would continuously force the circuit's voltage to follow the generated signal.

3.2 Resonator Electron Interaction

We have learned why we need the resonator to detect the electrons. However, this resonator also influences the behavior of the electrons.
When the particle induces an image current in the trap electrodes, a small voltage difference is generated across the detection circuit, resulting in an electric field that acts back on the electron. This back-action leads to a damping of the electron's motion and therefore causes its oscillation amplitude to decrease over time. If we consider this effect the electrons axial motion is not described as a free harmonic oscillator (2.9) but by a damped harmonic oscillation:

$$\ddot{z} + \gamma\dot{z} + \omega_z^2 z = 0 \quad , \tag{3.2}$$

where $\gamma = \frac{q^2 R_P}{m_e D^2}$ is the damping constant, R_P is the effective parallel resistance of the resonator, and D is the effective electrode distance. (see Appendix Sec. 5.3 for the derivation)
As a result of this damping, the electron continuously loses energy to the detection circuit. This effect can be used to cool the particle until it reaches thermal equilibrium with the resonator. This process is known as *resistive cooling*. The effective resistance of the resonator can be related to its quality factor Q by

$$R_P = Q\omega_{\mathrm{RLC}} L, \tag{3.3}$$

where Q is the quality factor of the resonator and ω_{RLC} is its resonance frequency. Therefore, the damping coefficient is proportional to the quality factor:

$$\gamma \propto Q.$$

Another definition for the quality factor Q is:

$$Q = \frac{f_{\mathrm{RLC}}}{\Delta f_{3\mathrm{dB}}}, \tag{3.4}$$

where f_{RLC} is the resonance frequency and $\Delta f_{3\mathrm{dB}}$ is the width at which the resonator response is reduced by 3dB relative to its maximum.

3.3 Driving and Coupling the Modes

As already mentioned in Sec. 2.6 the electrical field in the Penning trap is not perfect. This is a problem because it leads to the already described shifts and errors in the measurement. On the other hand we can use a deliberate variation of the field to manipulate the electrons in a specific way.
In our experiment we have a split correction electrode, where oscillating fields can be applied. Due to the geometry of the split electrode, the applied fields have a dipole as well as a quadrupole contribution and also higher order terms (see Appendix Sec. 5.1). Here we will have a closer look on how the oscillating dipole and quadrupole fields act on the particles in the trap. In general one can say that the dipole field drives the modes and the quadrupole field couples the different modes.

3.3.1 Driving the Modes

The split electrode can be used to create an oscillating dipole field e.g. in the z-direction, that oscillates with the excitation frequency ω_{ex}. This field is given by

$$\vec{E} = E_0 \, \Re(\exp(i\omega_{\text{ex}}t) \begin{pmatrix} 0 \\ 0 \\ 1 \end{pmatrix} \quad , \tag{3.5}$$

where E_0 describes the absolute strength of the field. The force excerted on a particle in the trap can then be described as

$$\vec{F} = q\vec{E} = qE_0 \, \Re(\exp(i\omega_{\text{ex}}t) \begin{pmatrix} 0 \\ 0 \\ 1 \end{pmatrix} \quad . \tag{3.6}$$

In addition in a real Penning trap we have two damping effects that limit the amplitude:

1. As the amplitude of the motion increases, the effects of the anharmonic imperfections of the trap become more significant, the effective frequency changes, the force goes out of resonance and the electrons are no longer driven by a driving force.
2. As the electrons move, they create induced currents in the circuit, which decay over time due to resistive losses. These image currents create a voltage difference across the endcaps which is out of the phase with the electron's motion and so counteracts it.

Therefore we get the equation of motion for the z-direction by adding the driving force as well as a damping term to Equation 2.9. We find

$$\ddot{z} + \gamma\dot{z} + \omega_z^2 z = \frac{q}{m} E_0 \, \Re(\exp(i\omega_{\text{ex}}t)) \quad , \tag{3.7}$$

where γ defines the damping coefficient, that depends on the factors described above.
We recognize this equation as a damped and driven harmonic oscillator. We know that on resonance ($\omega_{\text{ex}} = \omega_z$) the amplitude of the oscillation grows. Also integer multiples $\omega_{\text{ex}} = n\omega_z$ will excite the motion. Driving the z motion is useful because it increases the effects of the electrons on the circuit until their radius of motion becomes so large that they are lost from the trap. The loss of electron signal therefore indicates, that the excitation frequency ω_{ex} equals the axial frequency ω_z . Equivalently, other dipole terms in x- and y-direction can be used to drive and detect the magnetron ω_- and modified cyclotron frequency ω_+.

3.3.2 Coupling the Modes

The quadrupole part of the electrical field of the split electrode can couple different modes. We can see how this works by looking at the spatial dependence of the quadrupole field. One example for such a field is

$$\vec{E} = E_0 \begin{pmatrix} z \\ 0 \\ x \end{pmatrix} \Re\left(\exp(i\omega_{\text{ex}}t)\right) \quad . \tag{3.8}$$

The force that is exerted from this field is then given by

$$\vec{F} = qE_0 \begin{pmatrix} z \\ 0 \\ x \end{pmatrix} \Re\left(\exp(i\omega_{\text{ex}}t)\right) \quad . \tag{3.9}$$

We can see that when we plug this force into Equation 2.9, the equations of motion for the x- and z-direction are now coupled:

$$\begin{pmatrix} \ddot{x} \\ \ddot{y} \\ \ddot{z} \end{pmatrix} + \omega_c^2 \begin{pmatrix} -\dot{y} \\ \dot{x} \\ 0 \end{pmatrix} - \omega_z^2 \begin{pmatrix} x \\ y \\ -2z \end{pmatrix} = k_q \begin{pmatrix} z \\ 0 \\ x \end{pmatrix} \Re\left(\exp\left(i\omega_{\text{ex}}t\right)\right) \quad , \tag{3.10}$$

where we defined $k_q = \frac{qE_0}{m}$. A simplified version of these equations of motion are solved in the Appendix Sec. 5.2, but we already state the most important results here. First, we see that the equations of motion are now coupled together because coordinates appear in equations of motion other than their own (in addition to coupling of the x and y coordinates that is caused by the magnetic field in the trap). This changes the modes of motion. The effects are complicated, but practically the result is that there will be energy transfer between the modes (like two pendulums connected with a spring, resulting in an energy transfer between the modes). This energy transfer will be negligible (inefficient) for most excitation frequencies that we will choose and then the coupling terms will have no practical effect (like a very small spring constant in the earlier analogy). However, the calculation (see Appendix Sec. 5.2) reveals that specific excitation frequencies will create efficient energy transfer. It shows that if we choose the excitation frequency to be an integer multiple of either the sum or a difference of the frequencies of the two involved modes, efficient energy transfer will occur. Such sums or differences are called sidebands. The calculation shows that there are two types of efficient energy transfer: Rabi oscillations and exponential increase.

Rabi oscillations refer to a state where the amplitudes of the two modes change periodically, with a 90 degrees phase difference between them. For example, when coupling the z and the + modes like in this example with Rabi oscillations, the amplitude of the z motion will increase while that of the + motion will decrease, until the amplitude of the z motion will start decreasing again, at which point the amplitude of the + motion will start increasing and so on. If the amplitude is great enough this can cause the electrons to hit the trap electrodes and escape the trap.

Exponential increase is the state where both amplitudes increase exponentially. For example, when coupling the z and the + modes with exponential increase, the amplitude of each will increase exponentially. This will make the electrons hit the trap electrodes and escape it.

It follows from the calculation that for every pair of efficiently energy transferring frequencies, one of them will cause Rabi oscillations and the other will cause an exponential increase. For instance, $\omega_{\text{ex}} = \omega_z + \omega_+$ will cause Rabi oscillations while $\omega_{\text{ex}} = \omega_z - \omega_+$ will cause exponential increase.

Of course also other pairs of modes can be coupled by another quadrupole field. E.g. the + and - mode are coupled by a field

$$\vec{E} = E_0 \begin{pmatrix} y \\ x \\ 0 \end{pmatrix} \Re\left(\exp\left(i\omega_{\text{ex}}t\right)\right) \quad . \tag{3.11}$$

Coupling the motions is useful because we can use it to measure the frequencies of the motion ($\omega_{c,z,\pm}$) by using the following method: We can observe our electrons detection signal while exciting the split electrode with different frequencies. The electrons detection signal will remain roughly constant for most choices of the excitation frequency (because most excitation frequencies will create inefficient energy transfer and no electrons will be lost), however for certain frequencies it will drop significantly (because these excitation frequencies will cause

efficient energy transfer which will make at least one of the modes grow so large the electrons will hit the trap).
We can write down these frequencies, and, knowing that these frequencies are actually integer multiples of sums or differences of the frequencies of motion, we can extract the frequencies of motion from them.
To be able to do this we need to know which pair of frequencies of a given excitation frequency is a sum or a difference. (For instance, given that a certain frequency we found makes the electrons detection signal drop, we still don't know whether its $f_z - f_-$, or maybe $f_z + f_+$ and so on).
We can identify the pair by repeating the measurement with different ring voltages or coil currents. Different frequencies of motion have different dependencies on the ring voltage and the coil current, and so by observing whether and how a given excitation frequency shifted as a result of changing either the ring voltage or the coil current (or both), we can tell which frequencies of motion it is comprised of. In addition, we can calculate the frequencies to get an idea in which frequency range to look for them: $f_z - f_-$ for example will be much smaller than $f_z + f_+$.

Go back to the theory section, look at the formulas for the different frequencies and try to determine which parameters one needs to modify to cause them to shift, and in which direction.

The calculation that these results are based on is available at the appendix (see Sec. 5.2). You are not expected to know it by heart or to be able to reproduce it, but you should know the basic idea of how it goes.

Questions:

- What particles are we going to measure?
- How do charged particles get lost from containment?
- How does the detection system work, how do you measure the eigenfrequencies, what signal lineshape do you expect to get for trapped particles?
- Assuming that we continuously excite (give energy to) the axial mode, what happens when we efficiently couple it to another mode? Which frequencies do we expect to create efficient coupling?

4 Experiment

This chapter describes the experimental setup, the measurement control and the data analysis [Paasche, P. et al., 2002]. You will learn how to use professional measurement equipment, how to control experimental routines by software and about experimental techniques used in high-precision mass spectrometry.

4.1 Overview of the experimental setup

The Penning trap electrodes are mounted inside a vacuum chamber (10^{-8} mbar or better), pumped by a turbopump which is backed by a scroll pump. A cylindrical coil wrapped around the outside of the vacuum chamber generates the magnetic field. Electrical feedthroughs connect the electrodes inside the vacuum to the measurement electronics on the outside. The timing sequences are controlled by an Arduino single-board microcontroller, and data is read out by a PC.

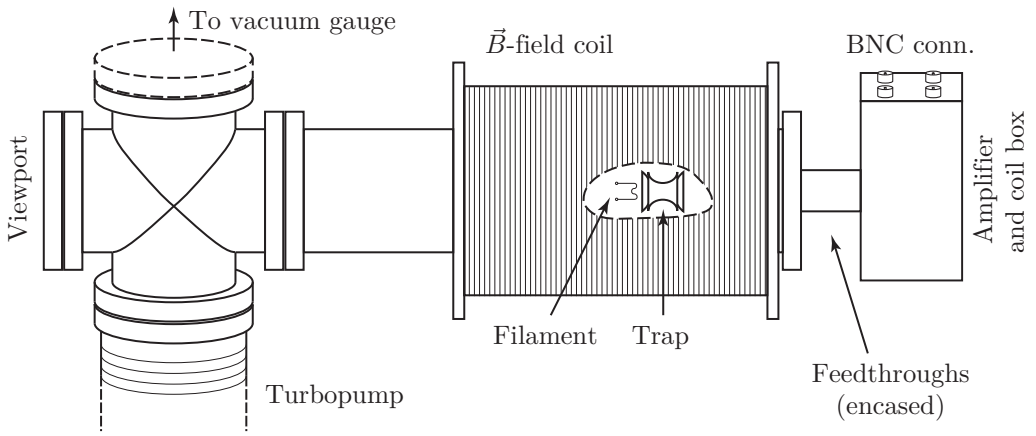


Figure 4.1: Overview of the experimental setup.

4.1.1 Mechanical setup

Connected to the ports of the CF63 cross are a viewport, a pressure gauge, the pumps and the vacuum tube that houses the Penning trap. Through the viewport, you can see the trap electrodes and the electron gun.
The Penning trap consists of five cylindrically shaped electrodes that are insulated from each other (Fig. 2.5).Next to the upper endcap[1] is the electron gun. The electrons are produced by thermal emission: A tungsten filament is heated by an electrical current running through it. When this filament is set to a negative voltage, electrons are repulsed from the filament through a grounded aperture plate (a plate with a hole in the middle) towards the trap. In this setup an additional plate is used to avoid switching the filament current on and off as this increases the risk of destroying the filament. Instead a 'blocking voltage' is applied

[1]The trap is mounted horizontally, but by convention, the endcap closer to the viewport is called "bottom endcap".

which blocks the electrons comming from the filament to the trap.
The electrons can enter the trap region through the hole in the anode (Fig. 2.5). These primary electrons cannot be trapped, since their energy is too high. Instead, secondary electrons, which are produced by collisions of the primary electrons with the residual gas, are trapped. During a measurement sequence with electrons in the trap, loading of further electrons is suppressed by switching the filament to ground potential. The lower the amplitude of the detecting dip signal, the more electrons we have in the trap. (We will learn how to do this in the next section).

4.1.2 Measurement electronics

Fig. 4.2 provides an overview over the Penning trap and the measurement electronics.
The magnetic field is generated by running a current of several 100 mA through a cylindrical coil. The current is controlled by a programmable power supply that can apply currents of up to $\approx 1.3\,\mathrm{A}$ through the coil's resistance of $\approx 50\,\Omega$.
The electrostatic trapping field is generated by applying a positive voltage to the ring electrode while the two endcaps are grounded DC-wise. A positive voltage is also applied to the correction electrodes, while AC signals are sent through the split correction electrode to excite the axial motion of the electrons. The ring electrode voltage is generated by a precision voltage source, which can be programmed or changed manually.
The radio-frequency excitation signal for the ω_{ex} is generated by a HP8657 signal generator. In order to apply the excitation during a well-defined period, the generator is not directly connected to the split electrode, but through a radio-frequency switch instead. The switch is closed for -5 V and open for 5 V, as in, if the voltage at the control port of the switch is -5 V, the RF generator signal goes into a $50\,\Omega$ resistor and nothing special happens, and if its 5 V, the RF generator signal goes to the split electrode. Thus, the excitation time and period can be defined by the length of the trigger pulse applied to the control port of the radio-frequency switch. In the measurement, you therefore need to plug in an excitation time in the code.
The current used to heat the filament for extracting electrons is provided by one of the 4 channels of the Hameg power supply. This channel "floats", meaning that neither the positive nor negative side of the channel are connected directly to ground. This allows the channel to be floated upwards or downwards (it can be "biased") by another, non-floating channel of the power supply. This filament bias voltage is applied through a fast HV-switch, which switches between the negative bias voltage and ground.
The coil and the low-noise amplifier of the axial-frequency detection system are enclosed in a metal box that is mounted on the outside of the vacuum system, onto the feedthrough flange. The supply voltages for the amplifier are provided by a 3-channel Hameg power supply.
The detection system, trap and cables form an *RLC*-circuit. It is connected to the DSA 815 network analyzer (spectrum analyzer, from now on SA) which excites it (and so the axial frequency of the electrons) when in Tracking Generator (TG) mode. The resulting voltage signal is amplified by a low-noise amplifier and given back to the SA as input. The trigger signals for the measurement sequence (loading the trap with ions, exciting them with the split electrode and starting the SA measurement) are generated by an Arduino-based trigger generator. An oscilloscope is used to visualize the trigger signals of the measurement sequence.

4.1.3 Measurement control

The experimental setup is controlled by a computer. You will receive a folder containing ready-made functions for controlling the setup, as well as an example file for setting up a basic measurement, which you will need to modify and expand. The scripts will save data into text files which can be viewed using Scilab (see shortcut on the desktop).

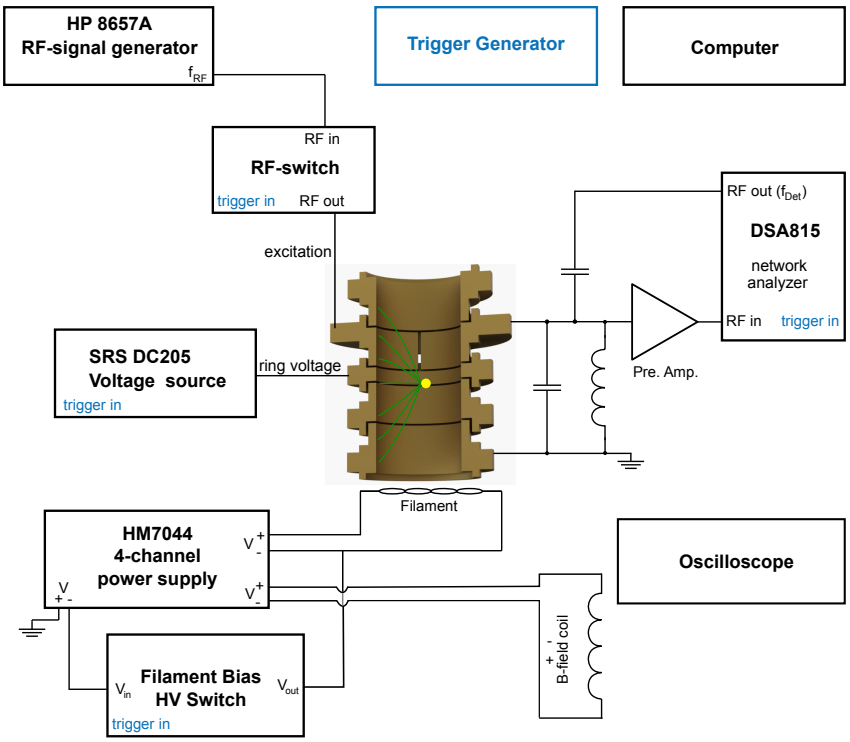


Figure 4.2: Overview of the measurement electronics.

The trapped electrons only remain trapped for a few 100ms, and are lost after they're measured (some are lost by the measurement process, which involves exciting them to the point where they are lost from the trap, while others collide with restgas. Therefore, in order to perform multiple measurements we need to continuously perform a cycle of loading new electrons, exciting them and detecting them.

The measurement scheme thus consists out of following steps (see Fig. 4.3):

1. Loading the trap (t_{load}, typ. 200 ms)
2. Waiting for voltages to stabilize (t_{wait1}, typ. 10 ms)
3. Exciting the electrons with ω_{ex} (t_{ex}, typ. 200 ms)
4. Additional waiting time (t_{wait2}, typ. 10 ms)
5. "Counting"/Detection of the electrons (this happens at the flank of the rigol trigger singal)
6. Expelling all electrons (This happens after waiting for a few seconds after the trigger signal is send).

Loading the trap: During the loading time the blocking voltage is set to zero, as described in Sec. 4.1.1, allowing electrons to reach the trap. The HV-switch used for switching the blocking voltage can be controlled by a TTL (5V) signal, which is generated by the trigger generator.

Excitation of the Electrons: As described in Sec. 4.1.2, ω_{ex} is not directly applied to the split electrode, but is instead connected to the input of an RF switch, which has its output

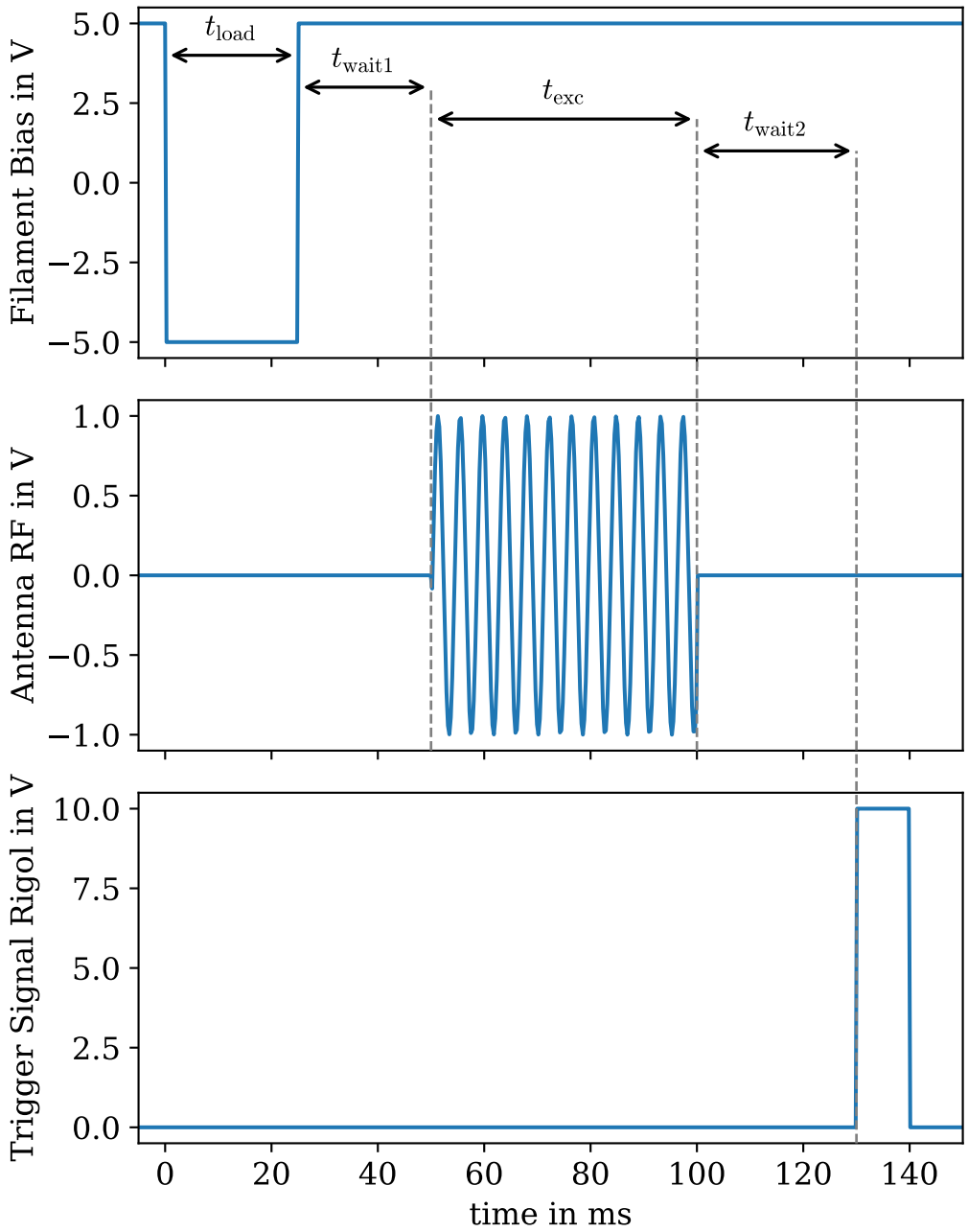


Figure 4.3: Timings of the measurement sequence. All times are controlled by the Arduino trigger generator. A dip is produced at the resonator frequency ν_{res}, if electrons are trapped.

connected to the split electrode. The switch is open (allows the signal to pass through the switch to the split electrode) when it gets 5V and is closed when it gets -5V. It can be controlled with a TTL signal which is generated by the trigger generator.

Counting/Detection of the Electrons: As explained in Sec. 3.1, when the electrons' axial frequency equals the RLC circuit's resonance frequency, the electrons short out the excitation signal, reducing its amplitude and signaling that we have electrons in the trap.
Just like how the trapped electrons create an induced signal in the circuit, so will an excitation signal running through the circuit apply induced forces on the trapped electrons. The effect of the excitation signal on the electrons will be insignificant unless its frequency is the same as the electron's resonance frequency, in which case it will give them energy, and lose energy itself due to conservation of energy.
Using this we can determine their frequency and the amount of electrons by fitting the dip of the signal of the RLC circuit. This dip has it's center at the frequency of the electrons and is broadened by the interaction with other electrons. One way to image this is by taking a look at the frequency of one single electron. The frequency is then well defined up to fluctuations of the Voltage supply. If more electrons are now trapped they will produce their own potential and move around effectively smearing out the trap potential leading to a broadening of the frequency.

4.2 Tasks

We will measure the different frequencies (reduced cyclotron, axial and magnetron, different sidebands) as a function of the coil current and the ring voltage and use the resulting graphs to measure different system parameters (go over the equations in the theory section and try to think which parameters can be extracted from such graphs). We will also measure the trapping time of electrons in the trap. Next, a detailed description of the measurement steps will be given. Keep in mind that original ideas are not only permitted, but encouraged.

4.2.1 Preparation

- The number of windings and the length of the coil are $N = (2400 \pm 30)$ and $L = (246.0 \pm 0.5)$mm, respectively. Assuming a long solenoid, calculate the magnetic flux density B as a function of the coil current I.
- To get a feeling for the motional frequencies, calculate the free cyclotron frequency ν_c of an electron for a magnetic flux density of the previously calculated coil for a current of $I = 1.3A$. You can look up the mass and charge of an electron for example on CODATA.
- Calculate the axial ν_z, magnetron ν_- and reduced cyclotron frequency ν_+ as a function of the ring voltage V_R for the previously calculated B-field and $C_2 = 1.4 \cdot 10^4 m^{-2}$. You can extract the C_2 coefficient by comparing Equation 2.7 and 2.18.
- Determine the needed Ring Voltage to set the axial frequency ν_z to 30MHz/50MHz/80MHz using the value for C_2 from above.

4.2.2 Identifying the Components

Before we start the measurements, get more familiar with the experimental setup by identifying the different devices shown in Fig. 4.2. Follow the cables and see what connects to what and try to understand what each device does. **Please don't plug/unplug any cables or change the values of the power supplies manually. This can mess up the experiment and even destroy certain components.** It's okay to change the coil

current remotely, using the computer. The devices you can manually operate are the Network Analyzer, the oscilloscope, the ring voltage and the HP8657A excitation power source. Feel free to play with them and fully explore their functionalities. Push lots of buttons, it's fun. Make yourself familiar with the minimum/maximum ratings given in Tab. 4.1.
A general note (relevant to all steps, not only this one): When the trap is not in use, the coil current should be 0.05A (arbitrary low value to prevent it from heating up significantly). **Therefore, at the end of each day in the lab before going home, if you're not performing a measurement, set the coil current to 0.05A, and if you are, make sure there is a line of code to change the coil current to 0.05A at the very end of your file, so that the coil can cool down after your script finishes running.**

4.2.3 Finding the detection system resonance frequencies and detecting electrons

Determine the resonance frequency of the axial resonator with the SA. If we knew the capacitance and the inductance, we could have calculated it outright (what is the formula for the resonance frequency of an *RLC*-circuit?), however, we don't. Therefore, play with the settings of the SA (frequency range, scale, trigger mode, ...) to find the resonance. The resonator coil is not shielded, therefore several resonances exist due to parasitic effects. You can zoom in to the plot by adapting the frequency range and center frequency. Use the marker for a better determination of the resonance frequency ν_{res} and note down its value. Make sure, the Tracking Generator (TG) is turned on. In this mode, the SA plots the same graph as before, but instead of relying on the input pulse alone in order to measure it, it sends pulses of its own with different frequencies (to the *RLC*-circuit) and measures the amplitudes of the returned pulses. (Why does this make the graph less noisy? See section 3.1 if you are not sure anymore.)
To figure out the best resonator for the upcoming measurements, you can ask yourself the following questions:

- In what range would you expect the RLC-circuit to have its resonance frequency? Hint: What is the maximum axial frequency that you can reach with the power supply?
- Which resonator has the least noise?

It is recommended to let the SA average over about 5 to 10 sweeps, to see a less noisy spectrum.
You should be left with 3 reasonable resonator signals. Now you can use the script **'Test.py'** (this can be done by opening the file with IDLE and pressing F5) to start a continuous sequence of loading the trap and taking measurements. You should adjust the following parameters:

- Ring voltage: Adjust the ring voltage depending to which resonator your currently looking at. This can be either done in the script with the function **set_ring_voltage()** or manually on the power supply on the table.
- Settings of the SA: To be able to see the dip signal better you should also adjust the settings of the SA. You can either use the functions **set_analyzer_center_span()** and **set_analyzer_ref_level()** in the script to zoom in onto the different resonators or use the buttons on the SA like before (this can be done by going back to local control by pressing the ESC button).

After examining the dip signals on the different resonators (do you even see a signal on all of the resonators?) one should have a better signal quality (good dip depth, little noise) than the others. Once you have identified the correct resonator zoom onto its resonance curve until you see about 10dB below the maximum of it.
Once you are satisfied with the image on the SA save the data. For this we provide a script named **'TakeMeasurement.py'**. Make sure to adjust the path and name in this script!

Table 4.1: Typical values and maximum-/minimum-ratings.

VALUE	DEVICE	TYP	MIN	MAX	UNIT
setup pressure	MaxiGauge	$5 \cdot 10^{-8}$	$5 \cdot 10^{-9}$	$1 \cdot 10^{-7}$	mbar
resevoir pressure	MaxiGauge	$3 \cdot 10^{-3}$			mbar
Coil Current	3CH Hameg	1.3	0.9	1.3	A
Coil Voltage	3CH Hameg	32.050			V
Filament Current	4CH Hameg	0.42		0.45	A
Blocking Voltage	4CH Hameg	72.0			V
Blocking Current	4CH Hameg	0.100			A
Acceleration Voltage	4CH Hameg	50.0			V
$\nu_{\text{excitation}}$	HP8657A		0.1	500	MHz
$\nu_{\text{excitation}}$ power	HP8657A	-10	-25	15	dBm
f_{det} power	DSA815	-30		-10	dBm
Ring Voltage	SRS DC205	20	0	100	V
RF Switch DC+	4CH Hameg	5	5	5	V
RF Switch DC−	4CH Hameg	-5	-5	-5	V
Amplifier Supply	3CH Hameg	3.4	3.4	3.4	V
Amplifier Gate 1	3CH Hameg	-0.84	-1.5	0	V
Amplifier Gate 2	3CH Hameg	-0.34	-1.5	0	V

4.2.4 Optimizing Measurement Paramters

After choosing the right resonator to perform the measurements with, we now want to optimize the measurement parameters. Try optimizing the depth of the dip by tuning the ring voltage and loading as well as the different waiting times. If the signal is still to weak for a proper measurement, ask your tutor so you can try to optimize the settings together. Also, move the electron dip across the resonator signal. What happens if the dip is on the side of the resonator curve? You should also use this opportunity to get a feeling for how the different parameters influence the signal you see to be able to choose reasonable values for the long term measurement at the end of the day. Especially also vary the coil current using the script (**set_coil_current()**). What happens if the coil current becomes too low? Note down some values of the coil current for which you can see a good signal to use them later in the long term measurement.

4.2.5 Measurement of the C_2 Coefficient

You have learned that the axial frequency of the trapped particle depends on the applied voltage and C_2-coefficient, where C_2 is a measure for the curvature of the electrostatic potential. To be more specific: the axial frequency $\omega_z \propto \sqrt{C_2 \cdot V_R}$.

This task aims to determine the experimentally realized C_2 coefficient of the trap used in the FP experiment. To do this, vary the applied voltage and measure the axial frequency as a function of the voltage. It is recommended to set the SA to average over multiple

measurements and use its marker function to read out the axial frequency. Take measurements using the **'TakeMeasurement.py** of at least three different voltages. If possible, take measurements at more than three voltages to obtain a more reliable fit.

Hint: Think about the dispersion of the dip when being off resonant to determine a more accurate frequency.

4.2.6 Electron trapping time measurement

The dip-width is a measure for the number of electrons in the trap, which drops exponentially with time. Open the **TrappingTime.py** script and adjust the times, coil current, ring voltage etc. Without any RF-excitations, vary the waiting time between loading and detection and take a measurement series for waiting time vs. signal amplitude (don't turn the RF-signal generator off, you can just turn off the output). **Make sure the data you record is useful. For this we provide another Script in the Trappingtime/Analysis folder with the name 'TrappingtimeAnalysis.py'. Run this script once to see if you get a reasonable plot as this is a good indicator for the Long-term measurement.**

4.2.7 Manual search for electron eigenfrequencies

Go back to the **Test.py** script. Use the RF-excitation to manually search for the axial, magnetron and modified cyclotron frequencies. Remember that you can calculate all frequencies to know in which range to look for them. If the excitation frequency matches a motional eigenfrequency, the electrons are ejected from the trap before the detection takes place and the dip vanishes. Write down a few frequencies that strongly affect the SA signal and don't forget to note other important parameters such as the coil current or the ring voltage.

Can you also find sidebands ($\nu_+ \pm \nu_-$ etc.)? Can you find multiples of an eigenfrequency? Find at least 5 different ones and test how strong your excitation has to be, to get a reasonable measurement.
Hint: The excitation Power is given in dBm. What does this mean?

4.2.8 Long-term measurement

Prepare a long-term measurement, which consists of three sets of measurements over a larger frequency range of 0MHz-500MHz (you can modify this range if you wish, as long as it stays reasonable). Vary the excitation amplitudes and coil currents, respectively, while leaving the voltage and number of averages fixed. Use the **ExcitationFrequencyScan.py**, adjust the important parameters as previously and write your code in the indicated region at the bottom of the script. This measurement will take one and a half days to complete and you will get the data once it's finished. **Make sure the measurement will be finished within 36h and remember to set the coil current back to** $0.05A$ **at the end of your measurement.** You can test this for example by running your code over a smaller frequency range with fewer steps and for only one set of parameters while stopping the time, and then extrapolate the time the whole measurement will take.

4.3 Data Analysis

1. Use the Data taken in 4.2.4. Determine the Q-Value of the Resonator by fitting. For this fit a Lorentzian to its lineshape. What are the benefits of having a resonator with a high/low Q-value?

2. Use the Data taken in 4.2.5. Subtract the Resonator signal which you fitted in the task before from the spectrum with dip and fit the dip using a Lorentzian, a Gaussian and a Voigt. Which of the fitting functions results in the most accurate frequency? Also think about how to estimate a reasonable error for the frequency.

3. Plot the axial frequencies as a function of the ring voltage and determine the C_2-coefficient by fitting the function you determined in the preparation tasks (don't forget the error). Use the CODATA values for the charge and mass of the electron. Do you see the expected behavior?

4. Try to identify the different lines from the long-term measurement. Use a symmetric function (e.g. a gaussian, lorentzian or voigt) to fit ν_+,ν_z, ν_-, ν_++ν_- and prepare a table containing all frequencies with estimated errors from the fits and their corresponding coil current, ring voltage and excitation amplitude. Remember that you can calculate the eigenfrequencies to get a feeling for where to look for them (or sidebands) in the plot. Also add the theoretically expected frequencies and the deviation from theory and measurement values in the table. Do your measured values agree with what you've calculated? What could be reasons for descrepancies?

5. Calculate the free cyclotron frequency from the sideband relation and using the invariance theorem. Do these values agree with each other? Do these values agree with the directly measured free cyclotron frequency $\nu_+ + \nu_-$? Do they agree with the theoretically calculated value? If this is not the case, what are possible reasons for the discrepancy? Extract the magnetic flux density from your data. Does it agree with your previous estimation?

6. Plot the free cyclotron frequencies (from the invariance theorem) as a function of the coil current. Do you see the expected behavior? Assuming that the length of the coil L is correct, determine the number of windings N.

7. Now turn the line of reasoning around. Assume that the coil parameters N, L are correct and extract the charge-to-mass ratio of the electron. Give a value for the electron mass by utilizing the CODATA value of the elementary charge.

8. Extract the decay constant / trapping time from the lifetime measurement: Assuming a linear dependence between dip-width and electron number, fit an appropriate function to the data. You can use the **Lifetime_Analysis.py** script.

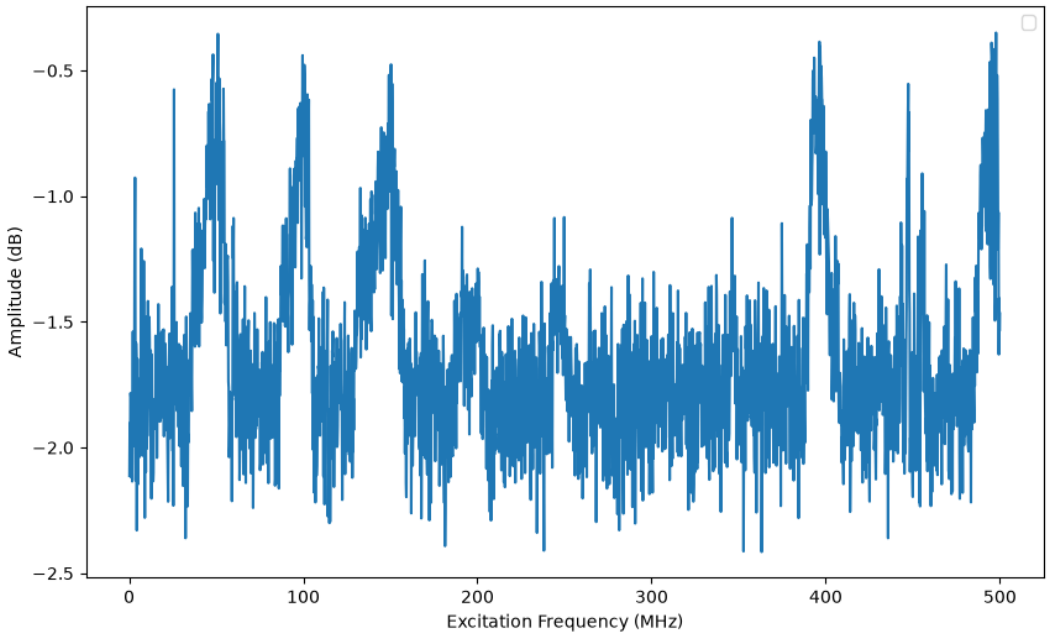


Figure 4.4: Typical scan over different rf-excitation frequencies applied to the split electrode for a fixed ring voltage, coil current and excitation power. The y-axis shows the dip depth of the electron signal.

5 Appendix A

5.1 Multipole Expansion

In this section we will go through a derivation of the multipole expansion of the electrical potential of the split electrode. We will see that it contains the dipole, quadrupole terms that we already refered to in Sec. 3.3.
Since the electrical field $\vec{E} = -\nabla\Phi$ has to fulfill the first Maxwell equation (Gauss's law)

$$\nabla \cdot \vec{E} = 0 \quad , \tag{5.1}$$

the potential in the trap has to fulfill the Laplace equation

$$\Delta\Phi = 0 \quad . \tag{5.2}$$

To describe the potential close to the trap center, we can start with a Taylor expansion about the origin

$$\Phi(\vec{x}) = \Phi(0) + \sum_i \frac{\partial\Phi}{\partial x_i}(0)x_i + \frac{1}{2}\sum_{ij}\frac{\partial^2\Phi}{\partial x_i \partial x_j}(0)x_i x_j + \cdots \quad , \tag{5.3}$$

where $\vec{x} = (x, y, z)$.
At this stage, the expansion is still completely general. However, because the potential satisfies Laplace's equation, the expansion coefficients are not independent. For example, the second-order derivatives satisfy

$$\frac{\partial^2\Phi}{\partial x^2}(0) + \frac{\partial^2\Phi}{\partial y^2}(0) + \frac{\partial^2\Phi}{\partial z^2}(0) = 0 \quad . \tag{5.4}$$

Analogous constraints apply to all higher-order terms. It is therefore convenient to rewrite the Taylor expansion in a basis of harmonic polynomials, i.e., polynomials that individually satisfy Laplace's equation. For the linear terms in Equation 5.3 this is trivial since all linear polynomials already satisfy the laplace equation. The easiest set of polynomials we can think of is

$$d_1 = x \tag{5.5}$$
$$d_2 = y \tag{5.6}$$
$$d_3 = z \quad . \tag{5.7}$$

Here we don't see a difference to the standard Taylor expansion. In the case of the quadratic terms in Equation 5.3 this is different. It is easily seen that one of the standard polynomials used in the Taylor expansion x^2 does not fulfill the Laplace equation:

$$\Delta x^2 = 2 \neq 0 \quad . \tag{5.8}$$

Therefore we need to find a new basis for the quadratic polynomials. Since the second derivative is symmetric with respect to an exchange of variables (the Jacobi matrix is symmetric), we need 6 independent polynomials. The constraint imposed by the Laplace

equation 5.4 removes one degree of freedom such that we are looking for a basis of 5 polynomials. Those are given by

$$q_1 = z^2 - \frac{x^2 + y^2}{2} \tag{5.9}$$

$$q_2 = x^2 - y^2 \tag{5.10}$$

$$q_3 = xy \tag{5.11}$$

$$q_4 = xz \tag{5.12}$$

$$q_5 = yz \quad . \tag{5.13}$$

It is easy to check that all of these polynomials are independent and satisfy the Laplace equation. With this information, we can rewrite the expansion of the potential as

$$\Phi(\vec{x}) = C + \sum_i a_i d_i(\vec{x}) + \sum_j b_j q_j(\vec{x}) + \ldots \quad . \tag{5.14}$$

This representation is known as the interior (inside the trap) multipole expansion, where a_i and b_j are the expansion coefficients. The contributions of the d_i polynomials are known as the dipole contributions and q_j are the quadrupole contributions. We can also find the terms that we saw in Sec. 3.3.2 are responsible for coupling between the modes. If we e.g. look at the field created by q_4 we find

$$\vec{E} \propto \nabla q_4 = \begin{pmatrix} z \\ 0 \\ x \end{pmatrix} \quad . \tag{5.15}$$

So if we apply a potential varying in time ($\propto \exp(i\omega t)$ on the split electrode we recover the coupling field from Equation 3.8.

5.2 Coupling the Modes

In this chapter we will go through the mathematical derivation for mode coupling in more detail (see Sec. 3.3.2). We will show that:

1. Efficient energy transfer between two modes occurs when the split electrode excitation frequency is chosen to be an integer multiple of a sum or a difference of the frequencies of the two coupled modes.

2. For every such pair (sum and difference) of frequencies, one will cause oscillations and the other will cause exponential increase.

The calculation is not rigorous but should still be somewhat convincing.

5.2.1 Coupling axial and cyclotron mode

As an example for the coupling of two modes, we have a look at the coupling of the axial and modified cyclotron modes in the trap. This coupling is induced by the quadrupole part of the electrical field in the trap which leads to a force on the particle given by

$$\vec{F} = qE_0 \begin{pmatrix} z \\ 0 \\ x \end{pmatrix} \Re\left(\exp\left(i\omega_{\mathrm{ex}} t\right)\right) \quad . \tag{5.16}$$

We can examine the effect of this force by plugging it into the equations of motion of a particle in the trap (see Equation 2.9). For simplicity, we will only consider the motion of the particle in the x and z direction, and treat both as independent harmonic oscillators. By

doing so, we neglect the coupling of the x and y coordinates by the magnetic field, which obviously leads to a different motion in the trap but for a qualitative understanding this treatment is sufficient. Starting with the equations of motion

$$\begin{aligned} \ddot{z} &= -\omega_z^2 z + \Re(k_q \exp(i\omega_{\text{ex}} t))x \\ \ddot{x} &= -\omega_+^2 x + \Re(k_q \exp(i\omega_{\text{ex}} t))z \quad , \end{aligned} \tag{5.17}$$

where we defined the new constant $k_q = \frac{qE_0}{m}$.
For a weak drive we can make the Ansatz:

$$\begin{aligned} z(t) &= \Re\left(\hat{z}(t)\exp(i\omega_z t)\right) \\ x(t) &= \Re\left(\hat{x}(t)\exp(i\omega_+ t)\right) \quad . \end{aligned} \tag{5.18}$$

Now we can derive the Ansatz two times where we assume that the amplitudes $\hat{z}(t)$ and $\hat{x}(t)$ change only slowly in time such that we neglect terms proportional to $\ddot{\hat{z}}(t)$ and $\ddot{\hat{x}}(t)$. We arrive at

$$\begin{aligned} \ddot{z}(t) &= \Re\left(-2i\omega_z \dot{\hat{z}}(t)\exp(i\omega_z t) - \omega_z^2 \hat{z}(t)\exp(i\omega_z t)\right) \\ \ddot{x}(t) &= \Re\left(-2i\omega_+ \dot{\hat{x}}(t)\exp(i\omega_+ t) - \omega_+^2 \hat{x}(t)\exp(i\omega_+ t)\right) \quad . \end{aligned} \tag{5.19}$$

This we now plug back into the equations of motion 5.17. We find two coupled differential equations for the amplitudes $\hat{z}(t)$ and $\hat{x}(t)$

$$\begin{aligned} \Re\left(-2i\omega_z \dot{\hat{z}}(t)\exp(i\omega_z t)\right) &= \Re\left(k_q \exp(i\omega_{\text{ex}} t)\right)\Re\left(\hat{x}(t)\exp(i\omega_+ t)\right) \\ \Re\left(-2i\omega_+ \dot{\hat{x}}(t)\exp(i\omega_+ t)\right) &= \Re\left(k_q \exp(i\omega_{\text{ex}} t)\right)\Re\left(\hat{z}(t)\exp(i\omega_z t)\right) \quad . \end{aligned} \tag{5.20}$$

Next we want to rewrite the real parts of the functions in the last equations as the sum of the complex number and the complex conjugate like

$$\Re(z) = \frac{1}{2}\left(z + z^*\right) \quad .$$

We get:

$$\begin{aligned} -\left(i\omega_z \dot{\hat{z}}(t)\exp(i\omega_z t) + \text{c.c.}\right) &= \frac{1}{4}\left(k_q \exp(i\omega_{\text{ex}} t) + \text{c.c}\right)\left(\hat{x}(t)\exp(i\omega_+ t) + \text{c.c.}\right) \\ -\left(i\omega_+ \dot{\hat{x}}(t)\exp(i\omega_+ t) + \text{c.c.}\right) &= \frac{1}{4}\left(k_q \exp(i\omega_{\text{ex}} t) + \text{c.c}\right)\left(\hat{z}(t)\exp(i\omega_z t) + \text{c.c.}\right) \quad . \end{aligned} \tag{5.21}$$

Here, "c.c." denotes the complex conjugate of the preceding term within the same set of parentheses. If we expand the product on the right-hand side of equations 5.21 we get 4 terms that oscillate with all possible combinations of ω_{ex} and, respectively, ω_+ and ω_z (since the complex conjugation of an oscillating term $\propto \exp(i\omega t)$ is proportional to $\exp(-i\omega t)$). Not all of these terms contribute to a solution of the differential equation and we will only keep the terms that have the biggest contribution to the solution. This is known as the Rotating-Wave-Approximation (RWA). To find out which terms we need to keep, we first notice that the left-hand side of the Equation 5.21 oscillates purely with ω_z or ω_+. We still assume that the amplitudes vary only slowly in time such that $\hat{z}(t)$ and $\hat{x}(t)$ don't have a substantial influence on the oscillation frequency. Therefore we require that both sides of the equation oscillate with the same frequency. From this consideration we can get two equations for the frequencies that solve Equation 5.21:

$$\begin{aligned} \omega_z &= \omega_{\text{ex}} \pm \omega_+ \\ \omega_+ &= \omega_{\text{ex}} \pm \omega_z \end{aligned} \quad . \tag{5.22}$$

We come to the conclusion that there are two possible excitation frequencies ω_{ex} that couple the two modes:

$$\omega_{\text{ex}} = \begin{cases} \omega_+ - \omega_z \\ \omega_+ + \omega_z \end{cases} . \tag{5.23}$$

We first examine the behavior for $\omega_{\text{ex}} = \omega_+ - \omega_z$: If we plug this into Equation 5.21 and only keep the terms that oscillate with ω_z (first line) or ω_+ (second line) and then multiply both sides with $\exp(-i\omega_z t)$ or $\exp(-i\omega_+ t)$ respectively, we find

$$\begin{aligned} i\omega_z \dot{\hat{z}}^*(t) &= \frac{k_q}{4}\hat{x}^*(t) \\ -i\omega_+ \dot{\hat{x}}(t) &= \frac{k_q}{4}\hat{z}(t) \end{aligned} . \tag{5.24}$$

Now we can derive and plug those two coupled equations (5.24) into each other and find the uncoupled equations

$$\begin{aligned} \ddot{\hat{z}}(t) &= -\frac{1}{16}\frac{|k_q|^2}{\omega_z\omega_+}\hat{z}(t) \\ \ddot{\hat{x}}(t) &= -\frac{1}{16}\frac{|k_q|^2}{\omega_z\omega_+}\hat{x}(t) \end{aligned} . \tag{5.25}$$

This we recognize as the differential equation of an oscillation with frequency

$$\Omega = \sqrt{\frac{1}{16}\frac{|k_q|^2}{\omega_z\omega_+}} . \tag{5.26}$$

Additionally, we can see from Equation 5.24 that there is a phase difference of $i = \exp(i\,\pi/2)$ between $\hat{x}(t)$ and $\dot{\hat{z}}(t)$ (and vice versa) from which we can see that the two solutions for $\hat{x}(t)$ and $\hat{z}(t)$ also have to have a phase difference of $\pi/2$. Depending on the initial conditions one solution could therefore be

$$\begin{aligned} \hat{z}(t) &\propto \cos(\Omega t) \\ \hat{x}(t) &\propto \sin(\Omega t) \end{aligned} . \tag{5.27}$$

Now we can also have a look at the second solution for ω_{ex}, the second line in Equation 5.23. We follow the same procedure as before: Plug in ω_{ex} in Equation 5.21 and only keep the terms on the right-hand side that oscillate with the same frequency as the left-hand side. Then we uncouple the equations by plugging them into each other and get

$$\begin{aligned} \ddot{\hat{z}}(t) &= \frac{1}{16}\frac{|k_q|^2}{\omega_z\omega_+}\hat{z}(t) \\ \ddot{\hat{x}}(t) &= \frac{1}{16}\frac{|k_q|^2}{\omega_z\omega_+}\hat{x}(t) \end{aligned} . \tag{5.28}$$

This looks like the equations 5.25 except that the sign is different. This subtle difference leads to a completely different behavior. The solutions to equations 5.28 are not oscillating, but exhibit an exponential increase or decrease

$$\begin{aligned} \hat{z}(t) &= C_1\exp(\Omega t) + C_2\exp(-\Omega t) \\ \hat{x}(t) &= C_1'\exp(\Omega t) + C_2'\exp(-\Omega t) \end{aligned} , \tag{5.29}$$

where the coefficients C_1, C_2, C_1' and C_2' depend on the initial conditions. Since the contribution from the exponentially decreasing term decreases, well, exponentially, for longer times the exponential increase dictates the behavior of both modes.

So in conclusion we saw that the two sidebands $\omega_{\text{ex}} = \omega_z \pm \omega_+$ can be excited by an external field. The two frequencies lead to a different behavior of the system: An excitation of the red sideband leads to oscillations, where the energy is stored alternating in both modes where as an excitation of the blue sideband leads to an exponential increase in the amplitude of both modes. In our experiment we can excite both sidebands with the split electrode and since both lead to an increase in the amplitude of the motion of the particle in the trap, we can detect that excitation by loosing the electron signal in the trap.

5.2.2 Other Couplings

Similar calculations can be done for the coupling of other modes. We find more sidebands at the sum and difference of each combination of modes. As we saw in the previous calculation, one of the combinations leads to oscillations and the other one to an exponential growth. Since the magnetron motion is not caused by a returning force like the cyclotron or axial motion, but rather by the $\vec{E} \times \vec{B}$-Drift (see Sec. 2.2), there is the difference that the sum of frequencies causes the oscillation rather than an exponential increase. In summary we have:

$$\omega_{\text{ex}} = \begin{cases} \omega_z + \omega_- & \text{oscillations} \\ \omega_z - \omega_- & \text{exponential increase} \\ \omega_+ + \omega_- & \text{oscillations} \\ \omega_+ - \omega_- & \text{exponential increase} \end{cases} \tag{5.30}$$

5.3 Resistive cooling

As discussed in Section 3.2, the oscillation of the electron induces an image current in the trap electrodes. This current generates a voltage across the detection circuit, which can be described by an effective resistance R_P. The resistance dissipates the electrical energy associated with the induced current as heat. The corresponding power loss is given by

$$\frac{dE}{dt} = -P = -I_{\text{img}}^2 R_P = -\frac{q^2 R_P}{D^2} \dot{z}^2, \tag{5.31}$$

where we have used the relation

$$I_{\text{img}} = \frac{q}{D} \dot{z}.$$

The total energy of the electron's axial harmonic motion is given by

$$E = \frac{1}{2} m_e \dot{z}^2 + \frac{1}{2} m_e \omega_z^2 z^2. \tag{5.32}$$

For a damped harmonic oscillator described by

$$\ddot{z} + \gamma \dot{z} + \omega_z^2 z = 0,$$

the rate of change of its mechanical energy is

$$\frac{dE}{dt} = -m_e \gamma \dot{z}^2. \tag{5.33}$$

Comparing the energy loss due to the detection circuit with the energy loss of the damped harmonic oscillator,

$$-\frac{q^2 R_P}{D^2} \dot{z}^2 = -m_e \gamma \dot{z}^2,$$

gives the damping coefficient

$$\boxed{\gamma = \frac{q^2 R_P}{m_e D^2}}. \tag{5.34}$$

Thus, the electrical energy dissipated in the effective resistance of the detection circuit corresponds directly to a damping force acting on the electron's axial motion.

5.4 Trap cabling and detection images

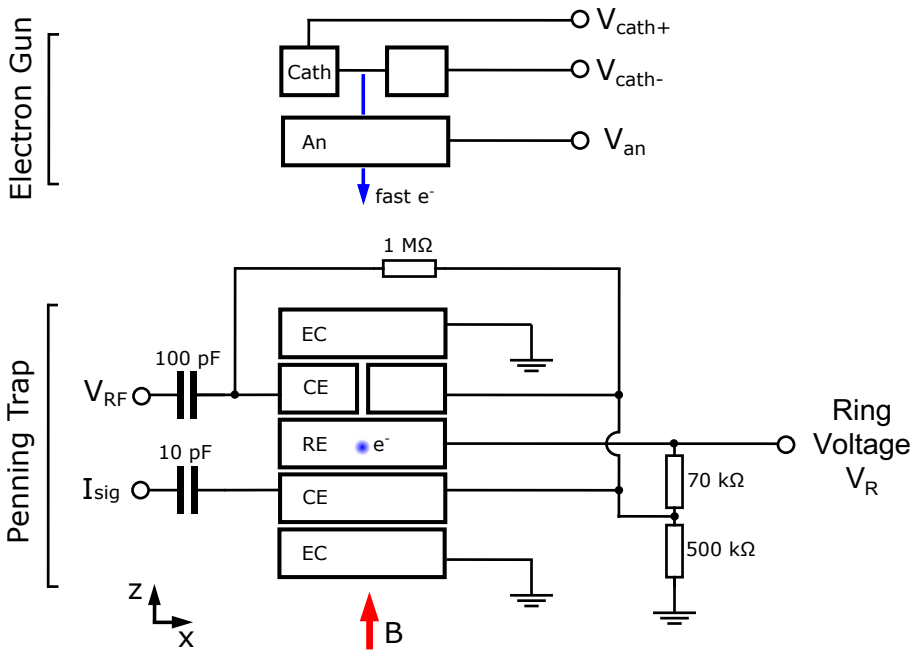


Figure 5.1: Trap cabling setup.

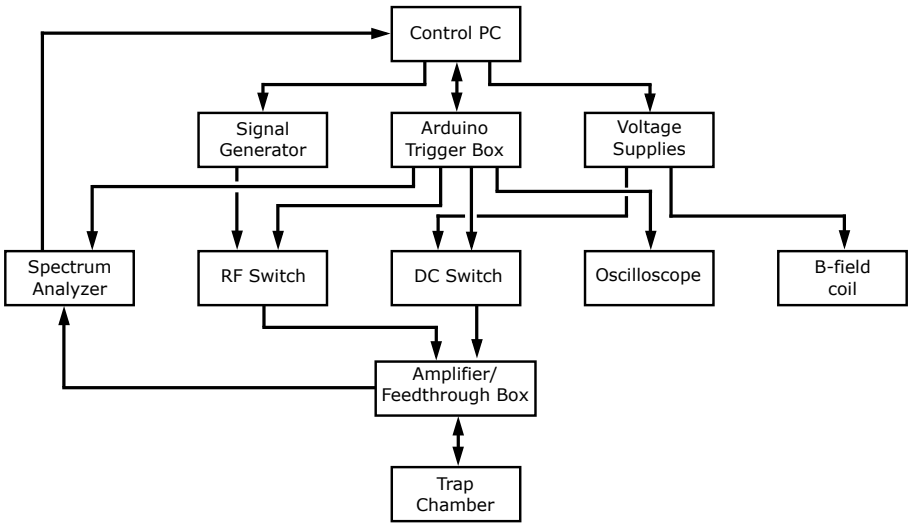


Figure 5.2: Overview of the measurement electronics and connections.

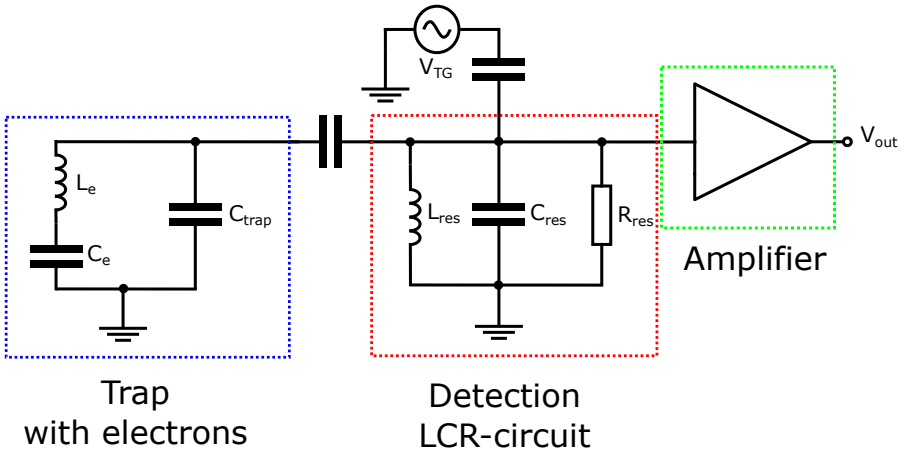


Figure 5.3: Schematic detection circuit.

Bibliography

K Blaum, H Kracke, S Kreim, A Mooser, C Mrozik, W Quint, C C Rodegheri, B Schabinger, S Sturm, S Ulmer, A Wagner, J Walz, and G Werth. g-factor experiments on simple systems in penning traps. *Journal of Physics B: Atomic, Molecular and Optical Physics*, 42(15):154021, jul 2009. doi: 10.1088/0953-4075/42/15/154021. URL https://doi.org/10.1088/0953-4075/42/15/154021.

Klaus Blaum. High-accuracy mass spectrometry with stored ions. *Physics Reports*, 425(1): 1–78, 2006. ISSN 0370-1573. doi: https://doi.org/10.1016/j.physrep.2005.10.011. URL https://www.sciencedirect.com/science/article/pii/S0370157305004643.

Lowell S. Brown and Gerald Gabrielse. Precision spectroscopy of a charged particle in an imperfect Penning trap. *Phys. Rev. A*, 25(4):2423–2425, 1982. doi: 10.1103/PhysRevA.25.2423. URL https://link.aps.org/doi/10.1103/PhysRevA.25.2423.

G. Gabrielse, L. Haarsma, and S. L. Rolston. Open-endcap Penning traps for high precision experiments. *International Journal of Mass Spectrometry and Ion Processes*, 88(2):319–332, 1989. ISSN 0168-1176. doi: 10.1016/0168-1176(89)85027-X. URL https://www.sciencedirect.com/science/article/pii/016811768985027X.

Paasche, P., Valenzuela, T., Biswas, D., Angelescu, C., and Werth, G. Individual and center-of-mass resonances in the motional spectrum of an electron cloud in a penning trap. *Eur. Phys. J. D*, 18(3):295–300, 2002. doi: 10.1140/epjd/e20020033. URL https://doi.org/10.1140/epjd/e20020033.

Stefan Ulmer, Klaus Blaum, and Wolfgang Quint. *Trapped charged particles: A graduate textbook with problems and solutions*. Advanced textbooks in physics. World Scientific, New Jersey and London and Singapore and Beijing and Shanghai and Hong Kong and Taipei and Chennai and Tokyo, 2016. ISBN 978-1-78634-011-5.